JACS
JOURNAL OF THE AMERICAN CHEMICAL SOCIETY
Communication
pubs.acs.org/JACS

Confined High-Pressure Chemical Deposition of Hydrogenated Amorphous Silicon

Neil F. Baril,[†,¶] Rongrui He,[†,¶] Todd D. Day,[†,¶] Justin R. Sparks,[†,¶] Banafsheh Keshavarzi,[‡] Mahesh Krishnamurthi,[§,¶] Ali Borhan,[‡] Venkatraman Gopalan,[§,¶] Anna C. Peacock,[#] Noel Healy,[#] Pier J. A. Sazio,[#] and John V. Badding*[,†,¶]

[†]Department of Chemistry, [‡]Department of Chemical Engineering, [§]Department of Materials Science and Engineering, and [¶]Materials Research Institute, Pennsylvania State University, University Park, Pennsylvania 16802, United States

[#]Optoelectronics Research Centre, University of Southampton, Highfield, Southampton SO17 1BJ, United Kingdom

Supporting Information

ABSTRACT: Hydrogenated amorphous silicon (a-Si:H) is one of the most technologically important semiconductors. The challenge in producing it from SiH_4 precursor is to overcome a significant kinetic barrier to decomposition at a low enough temperature to allow for hydrogen incorporation into a deposited film. The use of high precursor concentrations is one possible means to increase reaction rates at low enough temperatures, but in conventional reactors such an approach produces large numbers of homogeneously nucleated particles in the gas phase, rather than the desired heterogeneous deposition on a surface. We report that deposition in confined micro-/nanoreactors overcomes this difficulty, allowing for the use of silane concentrations many orders of magnitude higher than conventionally employed while still realizing well-developed films. a-Si:H micro-/nanowires can be deposited in this way in extreme aspect ratio, small-diameter optical fiber capillary templates. The semiconductor materials deposited have ~0.5 atom% hydrogen with passivated dangling bonds and good electronic properties. They should be suitable for a wide range of photonic and electronic applications such as nonlinear optical fibers and solar cells.

Hydrogenated amorphous silicon (a-Si:H) is produced on a very large scale for electronic and energy-related applications such as thin-film transistors and solar cells.[1,2] The SiH_4 precursor molecule typically used for a-Si:H deposition is thermodynamically unstable but does not pyrolize at an appreciable rate unless heated to temperatures >550 °C because of a significant kinetic barrier.[3,4] Conventional thermal pyrolysis techniques are therefore unsuitable for production of a-Si:H semiconductor films from SiH_4, as these temperatures are too high to allow for much hydrogen incorporation. Without hydrogen to passivate its dangling bonds, amorphous silicon has poor electronic and photonic properties.

The central challenge in depositing a-Si:H films is thus to overcome the kinetic barrier to decomposition at low enough temperatures; nonthermal plasmas that produce very reactive chemical species are commonly employed below atmospheric pressures.[1] Disadvantages of this plasma-enhanced chemical vapor deposition (PECVD)[1,2] approach include the considerable cost and complexity of the equipment needed to maintain a uniform plasma over large substrate areas and an inability to deposit conformally into deep trenches, pores, and other extreme aspect ratio templates, which is desirable for the fabrication of state-of-the-art nanomaterials, nanostructures, and nanodevices.[5] High reactant concentrations that activate silane decomposition via high rates of molecular collision could allow for increased reaction rates at a given temperature. However, in conventional reactors, high SiH_4 precursor concentrations lead to homogeneous nucleation and growth of undesired silicon nano-/microparticles in the gas phase rather than the desired heterogeneous deposition of films on substrates.[6,7]

We report that in reactors of microscale to nanoscale dimensions, such as small-diameter optical fiber capillaries, this difficulty can be overcome. Deposition in this manner (Figure 1a) allows for practical growth of uniform a-Si:H films (Figure 1b) without any particulate formation under SiH_4 partial pressures that are thus far as high as several megapascals (MPa). It is widely recognized that the scaling of the surface area to volume can have a major impact on the properties of nanosize objects. This scaling also has a large impact on the micro-/nanoreactors employed here, such that particulate formation is avoided.

The use of MPa SiH_4 partial pressures increases reaction rates by many orders of magnitude at temperatures that are low enough to allow for hydrogen incorporation. We find that a-Si:H film deposition rates of 3.7 Å s^{-1} (vs 1−10 Å s^{-1} for PECVD)[1] can be realized. The high-pressure approach is also advantageous in its efficient use of chemical precursors because minimal volumes of SiH_4 precursor are used in the microscale reactors and nearly all of it can be converted to silicon in the "closed" pore geometry described below. In contrast, the conversion efficiency for PECVD is typically significantly lower such that some fraction of the valuable silane precursor is wasted.[2] The minimal volumes of toxic and pyrophoric SiH_4 employed reduce the hazards associated with its use at high pressure.

Received: July 20, 2011
Published: December 8, 2011

   dx.doi.org/10.1021/ja2067862 | J. Am. Chem.Soc. 2012, 134, 19−22

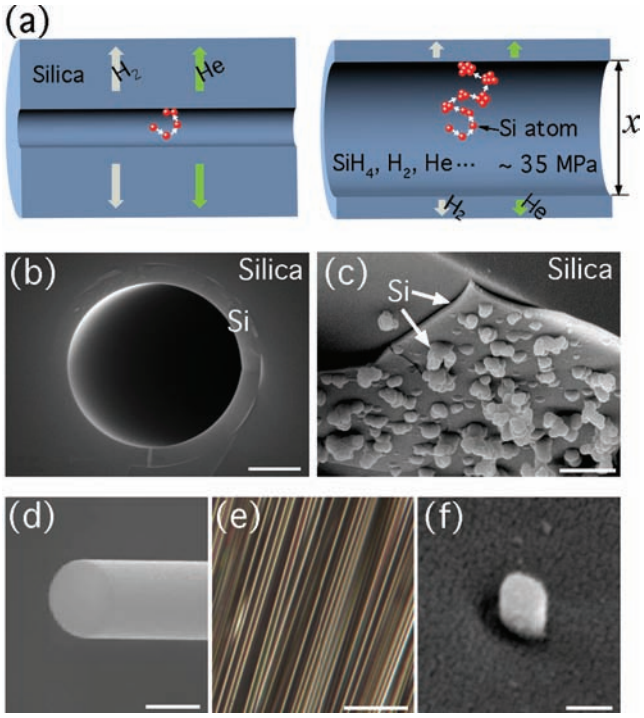

Figure 1. Deposition of a-Si:H wires and tubes. (a) Schematic of the high-pressure SiH_4 deposition process, showing the effect of a confined geometry. In micro-/nanopores (left) there is little time for silicon particles to nucleate and grow before reaching the pore walls, whereas in larger pores (right) there is enough time to produce clusters and then particles. He carrier and H_2 reaction byproduct diffuse directly through the silica walls. (b) SEM images of smooth a-Si:H film deposited in a 6 μm diameter silica capillary. (c) SEM image of a-Si:H film and particulates deposited in a 2500 μm diameter silica tube. (d) SEM image of a 6 μm diameter a-Si:H solid wire etched out of silica. (e) Optical micrograph of a bundle of 8 μm diameter a-Si:H wires that were deposited in parallel in a microstructured optical fiber template with many pores and subsequently etched out of it. (f) SEM image of a 280 nm diameter a-Si:H nanowire. Scale bars: (b) 2 μm, (c) 10 μm, (d) 5 μm, (e) 100 μm, (f) 300 nm.

To date, the only other reports of the fabrication of small-diameter a-Si:H wires involve the top-down approaches of etching a deposited film or traditional lithography.[8,9] While the bottom-up method of vapor–liquid–solid (VLS) growth is a common approach to the synthesis of semiconductor micro-/nanowires,[10] it appears to be incompatible with the growth of a-Si:H wires because crystalline silicon is formed from a saturated metal eutectic. The centimeters-long extreme aspect ratio pores in the optical fiber capillaries used for high-pressure deposition have ~1 Å root-mean-square surface roughness.[11] More complex microstructured optical fibers can be drawn with hundreds to thousands of pores with diameters ranging from tens of micrometers to <10 nm. These pores can be arranged in precisely defined patterns with a wide range of different symmetries to form extreme aspect ratio silica micro-/nanotemplates.[12,13] Thus, using the approach reported here, near atomically smooth a-Si:H wires can now be hierarchically organized at length scales from micrometers to nanometers in a single optical fiber to exploit their excellent electronic and photonic properties.

Silica fiber capillaries ranging from 280 nm to 2500 μm in diameter with 60–100 μm thick walls were drawn at the University of Southampton optical fiber fabrication cleanroom facility and used as reactors to carry out the high-pressure a-Si:H deposition. SiH_4 at 1.7 MPa partial pressure mixed with 33.3 MPa of helium carrier gas was configured to flow in the capillaries (see Supporting Information (SI)), which were heated in a furnace to 400–420 °C to induce deposition (Figure 1a,b). Two experimental configurations were used in which the end of the capillary opposite the gas inlet was either open to allow for gas flow or sealed closed to inhibit it. In both cases, well-developed films were formed when the capillary diameter was confined to <300 μm. When a larger 2500 μm internal diameter capillary was used for deposition under the same reaction conditions used for smaller pores, undesired silicon particles were formed along with a film (Figure 1c). We observed that larger reactors with dimensions on the order of centimeters produced predominantly particles ("fines"), in agreement with previous reports.[6] On the basis of these observations, we conclude that in the confined geometry, any particles that form homogenously have little time to grow into larger particles before reaching the pore walls and becoming embedded in the growing film. The time required for a nucleated particle to reach the pore wall scales as x^2/D, where x is the pore diameter and D is the gas-phase diffusivity of the particle. x^2/D is orders of magnitude smaller in the 6 μm pores than in ≥300 μm pores (Figure 1a). Confined high-pressure deposition can continue on the interior of the tube until centimeters-long void-free wires are formed (Figure 1d). Many wires can be formed in an array of silica pores (Figure 1e) at dimensions down to the nanoscale (Figure 1f). The results of these experiments, showing formation of a-Si:H at low temperatures, suggest that confinement also plays a role in avoiding particle formation in higher temperature high-pressure depositions that form hydrogen-poor amorphous silicon or germanium, or crystalline silicon or germanium in fiber pores.[12] The heterogeneous deposition of well-developed films, instead of the formation of homogeneously nucleated particles, in these high-pressure experiments previously has not been fully understood.

Secondary ion mass spectrometry analyses for the wires deposited at 400–420 °C in the sealed capillaries gave a hydrogen concentration of 0.5 atom%, although as much as 1–2% cannot be ruled out (see SI). Furthermore, these wires have Raman and infrared spectra (Figure 2) exhibiting vibrational

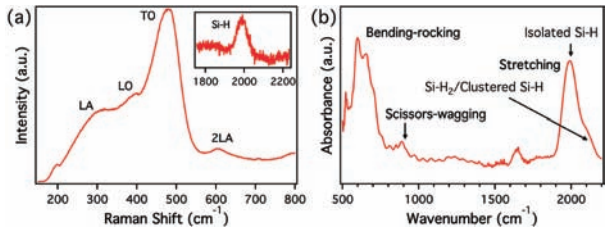

Figure 2. (a) Raman spectrum collected with 633 nm excitation, showing the characteristic longitudinal acoustic (LA), longitudinal optical (LO), transverse optical (TO), and second-order longitudinal acoustic (2LA) vibrational modes of a-Si and the Si–H stretch mode near 2000 cm^{-1} (inset). (b) IR spectrum of an a-Si:H wire collected using a Fourier transform infrared microscope in the reflection geometry.

modes of characteristic of silicon–hydrogen bonds. Based on the ratio of integrated band intensity between the 2000 and 2090 cm^{-1} stretching IR modes, the isolated Si–H bonding accounts for ~76% of the hydrogenation configuration, with

dx.doi.org/10.1021/ja2067862 | J. Am. Chem.Soc. 2012, 134, 19–22

the rest being polyhydride bonds (e.g., Si−H_2) or clustered Si−H. In contrast, material deposited at a higher temperature of 500 °C had no Si−H or Si−H_2 modes.

The gas-phase unimolecular decomposition reaction 1 is generally considered to be the first step in the pyrolysis of silane in thermal CVD, except at very low pressures.[3,4]

$$SiH_4 \rightarrow SiH_2 + H_2 \quad (1)$$

SiH_4 is a small molecule with no low-frequency vibrational modes,[3] whose reaction kinetics in reaction 1 are in the falloff region at pressures used for conventional low-pressure CVD (LPCVD).[15] High pressures should thus accelerate the decomposition because of the greatly increased frequency of molecular collisions. The high-pressure reaction kinetics of the pyrolysis of pure SiH_4 (to form a-Si:H particles) have previously been investigated,[14] but no experimental data for SiH_4 in a high-pressure He bath relevant to the present confined deposition experiments have been reported.[15] Given the relative partial pressures of SiH_4 and He employed, most of the molecular collisions will involve helium. Using the Troe form of the parametrized rate falloff of reaction 1 determined from quantum Rice−Ramsperger−Kassel (QRRK) calculations[15] at a temperature of 420 °C, it can be predicted (Figure 3) that the unimolecular rate constant increases from 1.6 × 10^{-7} s^{-1} at 13 Pa, a pressure typically employed for LPCVD experiments,[16] to 4.6 × 10^{-4} s^{-1} at 10 MPa, the high-pressure limit.[15] Thus, at high pressure, the rate of reaction 1 increases (when compared with LPCVD) because of both the ∼10^5-fold increase in SiH_4 concentration (13 Pa vs 1.7 MPa) and the ∼10^3-fold increase in the rate constant. Although surface reactions may be rate limiting, it appears likely that the increased rate of production of SiH_2 in the gas phase will increase the film deposition rate. Indeed, at 450 °C, the deposition rate was reported to be 0.01 Å s^{-1} for LPCVD with a SiH_4 pressure of 13 Pa,[16] while in our high-pressure CVD experiments in an open capillary, a 30-fold increase to a rate of ∼0.3 Å s^{-1} was observed with a SiH_4 partial pressure of 1.7 MPa. Quantitatively accounting for the effect of high pressure on deposition rates would require a detailed modeling study of 30 or more coupled reactions that occur after SiH_2 production to ultimately deposit a-Si:H.[3,4,14] The collision-induced acceleration of the rate of reaction 1 is illustrative of what could happen to many of these subsequent reactions under high pressure to accelerate the overall deposition rate. Deposition rates as a function of time were determined experimentally by stopping successive identical depositions at different times and measuring the film thicknesses using scanning electron microscopy (see SI).

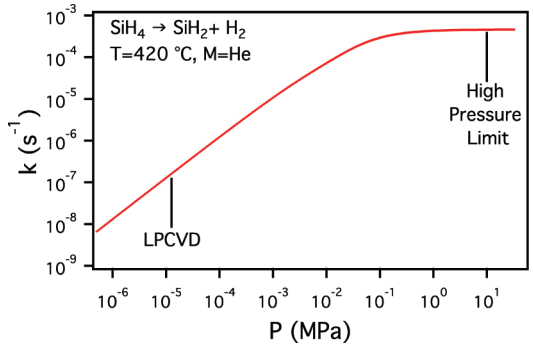

Figure 3. First-order rate constant vs pressure for unimolecular reaction of SiH_4 to produce SiH_2 and H_2 in a He bath determined from QRRK calculations.[15] The *x* axis represents the total pressure, the sum of the precursor and bath gas partial pressures. LPCVD is performed at a pressure (1.3 × 10^{-5} MPa) in the falloff region where the rate constant is decreasing with decreasing pressure. The micro-/nanoreactor depositions are performed at He pressures well above the high-pressure limit of ∼10 MPa.

When the end of the silica capillary is sealed closed to inhibit pressure-driven flow, the deposition rate accelerates. As an example, at 420 °C, the rate is ∼0.08 Å s^{-1} for an open pore, whereas for a closed pore it is as high as 3.7 Å s^{-1} (see SI). For comparison, under conventional thermal CVD conditions (13 Pa pressure) at 420 °C, the growth rate predicted using the reported activation energy of 164 kJ mol^{-1} is 0.004 Å s^{-1},[16] 925 times slower.

This observation is counterintuitive because, in the absence of pressure-driven flow, consumed SiH_4 would not be expected to be replenished except by the very slow molecular diffusion process. The observed increase in rate can be explained by the ability of silica pore walls to enhance the concentration of the SiH_4 precursor (and also the concentration of silicon hydride reaction intermediates) relative to the He carrier and H_2 reaction byproduct. Silica at temperatures of several hundred °C is permeable to H_2 and He, but not to SiH_4.[17] Thus SiH_4 is driven into the pore from the high-pressure precursor reservoir and trapped as He and H_2 exit through the pore walls. Modeling predicts (see SI) that the partial pressure of SiH_4 in the region of the capillary at 420 °C is raised from its initial value of 1.7 to 3.4 MPa. The phenomenon observed in this particular case implies that higher growth rates can be achieved by increasing silane pressures and closing the pore. We have previously shown that the precursor filtering capability of silica allows for the void-free filling of fiber pores with silicon and germanium,[17] which we now observe for a-Si:H (Figure 1d,f) over a distance of 5 cm, as determined by sectioning the wire every 0.5 cm and collecting cross-sectional SEM micrographs. When the pore is open, all of the gases in the precursor mixture can exit, so the SiH_4 concentration is not selectively enhanced. The selective filtering effect of the silica micro-/nanoreactor walls in the closed pore geometry also allows for a nearly 100% conversion efficiency because the H_2 byproduct is continuously removed and the SiH_4 precursor is continuously replenished; the thermodynamic driving force for the forward reaction 1 is thus sustained, in contrast to the behavior for a chemical bath in conventional closed system with nonpermeable walls.

Typical PECVD films require hydrogen contents of 5−10 atom% for good passivation of electronic defects.[2] In contrast, we find that ∼0.5 atom% hydrogen can passivate defects in the a-Si:H films deposited at high pressure such that they exhibit good semiconducting properties. Excellent properties are also observed for relatively low hydrogen content in a-Si:H deposited by hot wire CVD, so there is precedent for materials passivation at low hydrogen contents.[2] Key indicators of a-Si:H semiconductor materials quality include its optical loss, dark and illuminated conductivity, and carrier activation energy.[2] The optical losses at 1.55 μm wavelength are 0.4 cm^{-1} determined by a standard cutback method[18] on materials deposited in fiber pores to form a-Si:H optical waveguides. In comparison, an absorption coefficient of ∼0.1 cm^{-1} is typical of "device quality" a-Si:H deposited via PECVD.[19] Light at 1.55 μm has an energy of 0.8 eV, which is in the middle of the a-Si:H bandgap. Thus, the low optical loss at this wavelength is an indication of a low density of unpassivated defects in the gap.

dx.doi.org/10.1021/ja2067862 | J. Am. Chem.Soc. 2012, 134, 19−22

Furthermore, the dark electrical conductivity is measured to be 9.2×10^{-11} Ω^{-1} cm^{-1} (Figure 4a), within the range of $<1 \times 10^{-10}$ Ω^{-1} cm^{-1} required for device-quality a-Si:H. The wires are also highly photoconductive, as an increase of several orders of magnitude in the conductivity is observed when they are illuminated with 633 nm light (Figure 4a). This significant photoresponse demonstrates their potential application as active absorbers in solar cells, which are now being fabricated in wire or "pillar array" geometries.[20] The electrical conductivity of the deposited a-Si:H also increases with increasing temperature as more carriers are thermally excited. An Arrhenius fit (Figure 4b) reveals an activation energy of 0.8 ± 0.02 eV, compared with ~0.8 eV for device-quality a-Si:H. Thus, the deposited a-Si:H has considerable promise for electronic applications.[2] Good-quality a-Si:H materials that have low hydrogen content may be less susceptible to the light-induced degradation known as the Staebler–Wronski effect.[21] The high proportion of isolated Si–H bonds revealed by IR spectroscopy may also be advantageous to materials performance, as a decreased electronic density of states and reduced susceptibility to the Staebler–Wronski effect have been observed for materials with higher monohydride to polyhydride ratios.[1,2] The decrease in efficiency over time of a-Si:H solar cells arising from the Staebler–Wronski effect represents a significant barrier to their widespread adoption.[2]

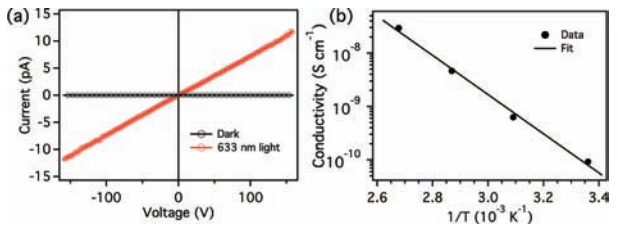

Figure 4. Electrical characterization of a 6 μm diameter a-Si:H microwire. (a) Current–voltage curves measured in the dark and under illumination with 633 nm light at a power density of 87 mW cm^{-2}. The ratio of the photoconductivity to dark conductivity is 1200. (b) Temperature dependence of dark conductivity.

We have demonstrated that a-Si:H can be deposited from very high pressures of silane in a confined geometry to form micro- and nanowires of a-Si:H. Without confinement, undesired homogeneous nucleation and growth of large numbers of particles occurs at such high silane pressures. Conventional a-Si:H deposition approaches, such as PECVD or hot wire CVD, have not been reported to deposit well-developed structures in extreme aspect ratio micro-/nanoscale voids or templates. The high rate of molecular collisions at high pressure greatly increases the rate of deposition over that found at pressures below 0.1 MPa to practical values exceeding 1 Å s^{-1}. The properties of the deposited wires make them promising candidates for optical fiber devices, solar cells, and other types of applications. The nonlinear optical properties of a-Si:H, for example, are superior to those of crystalline silicon,[22] making a-Si:H wires embedded in optical fiber capillaries potentially useful for high-speed optical switching applications.

■ ASSOCIATED CONTENT

Supporting Information

Deposition apparatus, deposition rates, SIMs measurements, and modeling. This material is available free of charge via the Internet at http://pubs.acs.org.

■ AUTHOR INFORMATION

Corresponding Author

jbadding@chem.psu.edu

■ ACKNOWLEDGMENTS

We acknowledge funding from EPSRC (EP/G028273/1), the National Science Foundation, DMR-0820404, DMR-0507146, and the Penn State Materials Research Science and Engineering Center, funded by NSF award DMR-0820404. A.C.P. is a holder of a Royal Academy of Engineering fellowship.

■ REFERENCES

(1) Street, R. A. *Hydrogenated Amorphous Silicon*; Cambridge University Press: Cambridge, 1991.

(2) Schropp, R. E. I.; Zeman, M. *Amorphous And Microcrystalline Silicon Solar Cells: Modeling, Materials And Device Technology*; Kluwer Academic: Boston, 1998.

(3) Jasinski, J.; Gates, S. *Acc. Chem. Res.* **1991**, *24*, 9–15.

(4) Giunta, C.; McCurdy, R.; Chapplesokol, J.; Gordon, R. *J. Appl. Phys.* **1990**, *67*, 1062–1075.

(5) Martin, C. R. *Chem. Mater.* **1996**, *8*, 1739–1746.

(6) Odden, J. O.; Egeberg, P. K.; Kjekshus, A. *J. Non-Cryst. Solids* **2005**, *351*, 1317–1327.

(7) Jones, A. C.; Hitchman, M. L. *Chemical Vapour Deposition: Precursors, Processes And Applications*; Royal Society of Chemistry: Cambridge, UK, 2009.

(8) Zhu, J.; Yu, Z. F.; Burkhard, G. F.; Hsu, C. M.; Connor, S. T.; Xu, Y. Q.; Wang, Q.; McGehee, M.; Fan, S. H.; Cui, Y. *Nano Lett.* **2009**, *9*, 279–282.

(9) Cantley, K. D.; Subramaniam, A.; Pratiwadi, R. R.; Floresca, H. C.; Wang, J.; Stiegler, H.; Chapman, R. A.; Kim, M. J.; Vogel, E. M. *Appl. Phys. Lett.* **2010**, *97*, 143509.

(10) Duan, X.; Lieber, C. *Adv. Mater.* **2000**, *12*, 298–302.

(11) Roberts, P.; Couny, F.; Sabert, H.; Mangan, B.; Birks, T.; Knight, J.; Russell, P. *Opt. Exp.* **2005**, *13*, 7779–7793.

(12) Sazio, P. J. A.; Amezcua-Correa, A.; Finlayson, C. E.; Hayes, J. R.; Scheidemantel, T. J.; Baril, N. F.; Jackson, B. R.; Won, D.-J.; Zhang, F.; Margine, E. R.; Gopalan, V.; Crespi, V. H.; Badding, J. V. *Science* **2006**, *311*, 1583–1586.

(13) Monro, T. M.; Ebendorff-Heidepriem, H. *Annu. Rev. Mater. Res.* **2006**, 1–31.

(14) Odden, J.; Egeberg, P.; Kjekshus, A. *Int. J. Chem. Kinet.* **2006**, *38*, 309–321.

(15) Dollet, A.; de Persis, S.; Teyssandier, F. *Phys. Chem. Chem. Phys.* **2004**, *6*, 1203–1212.

(16) Manfredotti, C. *Thin Solid Films* **1986**, *141*, 171–178.

(17) Baril, N. F.; Keshavarzi, B.; Sparks, J. R.; Krishnamurthi, M.; Temnykh, I.; Sazio, P. J. A.; Peacock, A. C.; Borhan, A.; Gopalan, V.; Badding, J. V. *Adv. Mater.* **2010**, *22*, 4605–4611.

(18) Feng, X.; Monro, T. M.; Petropoulos, P.; Finazzi, V.; Hewak, D. *Opt. Exp.* **2003**, *11*, 2225–2230.

(19) Harke, A.; Krause, M.; Mueller. *J. Electr. Lett.* **2005**, *41*, 1377–1379.

(20) Fan, Z.; Ruebusch, D. J.; Rathore, A. A.; Kapadia, R.; Ergen, O.; Leu, P. W.; Javey, A. *Nano Res.* **2009**, *2*, 829–843.

(21) Staebler, D. L.; Wronski, C. R. *J. Appl. Phys.* **1980**, *51*, 3262–3268.

(22) Narayanan, K.; Elshaari, A. W.; Preble, S. F. *Opt. Exp.* **2010**, *18*, 9809–9814.